Received: 13 October 2023 | Revised: 22 March 2024 | Accepted: 6 April 2024

DOI: 10.1002/jcb.30569

RESEARCH ARTICLE

Journal of Cellular Biochemistry WILEY

HN1 is a novel dedifferentiation factor involved in regulating the cell cycle and microtubules in SH-SY5Y neuroblastoma cells

Tilbe Özar | **Aadil Javed** | **Gülseren Özduman** | **Kemal S. Korkmaz**

Cancer Biology Laboratory, Department of Bioengineering, Faculty of Engineering, Ege University, Izmir, Turkey

Correspondence
Kemal S. Korkmaz
Email: ks_korkmaz@yahoo.com and kemal.sami.korkmaz@ege.edu.tr

Present address
Aadil Javed, Aadil Javed, Department of Molecular, Cellular and Developmental Biology (MCDB), University of Michigan, Ann Arbor, MI, USA.

Funding information
Ege University BAP project, Grant/Award Number: FGA-23341; TÜBİTAK Project, Grant/Award Number: 221Z202

Abstract

Hematological and neurological expressed 1 (*HN1*), encoding a small protein, has been recently explored in different cancers owing to its higher expression in tumor samples as compared to adjacent normal. It was discovered and subsequently named because of its higher expression in hematological and neurological tissues in developing mice. Following discovery, it was considered a neuronal regeneration or dedifferentiation-related gene. However, since then, it has not been characterized in neuroblastoma or differentiated neurons. SH-SY5Y cell line presents a unique model of neuroblastoma often utilized in neurobiology research. In this study, first, we employed bioinformatics analysis along with in vitro evaluation using normal and retinoic acid (RA)-differentiated SH-SY5Y cells to determine the responses of HN1 and its function. The analysis revealed that *HN1* expression is higher in neuroblastoma and lower in differentiated neurons and Parkinson's disease as compared to appropriate controls. Since HN1 coexpression network in neuroblastoma is found to be enriched in cell-cycle-related pathways, we have shown that HN1 expression increases in S-phase and remains lower in the rest of the cell cycle phases. Moreover, HN1 expression is also correlated with the microtubule stability in SH-SY5Y cells, which was investigated with nocodazole and taxol treatments. *HN1* overexpression increased the ratio of S-type cells (undifferentiated), indicating that it acts as a dedifferentiating factor in neuroblastoma cells. Moreover, cell cycle dynamics also changed upon *HN1* overexpression with alternating effects on SH-SY5Y and RA-differentiated (N-type) cells. Therefore, *HN1* is a potential cell cycle regulatory element in the development of neuroblastoma or dedifferentiation of neurons, which requires further studies to decipher its mechanistic role.

KEYWORDS
cell cycle, differentiation, HN1, microtubules, neuroblastoma, retinoic acid

1 | INTRODUCTION

The *hematological and neurological expressed 1* (HN1) gene encodes a 154 amino acid protein which has been named after the discovery of its specific expression in tissues of hematological and neurological origins in mice in 1997.[1] HN1 messenger RNA (mRNA) levels are recorded as higher in the developing nervous system as compared to the adult brain, implicating the role of *HN1* in the development of the nervous system. Furthermore, in a model of motoneuron regeneration of mice and rats, it was upregulated in injured facial motoneurons indicating a role in nerve regeneration.[2] A dedifferentiation model of retinal pigment epithelial (RPE) cells from Newt (*Cynops pyrrhogaster*) retina removal and subsequent observation of reconstruction of the neural retina showed that *HN1* is expressed in dedifferentiating and progenitor cells of the retina.[3] It was deduced that HN1 might play a role in the dedifferentiation of RPE cells. In melanoma cells, *HN1* silencing led to increased melanogenesis and the expression profile of differentiation markers and considering previous literature at the time, it was assumed that *HN1* acts as a suppressor of differentiation in proliferating cells.[4] Later, it was also shown that *HN1* expression was correlated with depigmentation of RPE cells in a model of regeneration of Newt retinal development. The researchers deduced that *HN1* could be useful in determining dedifferentiated cells from differentiated ones in the models of regeneration and development.[5] However, no studies were further conducted to understand the role of *HN1* in the dedifferentiation of neurons in higher animals such as mammals or vertebrates considering that HN1 is highly conserved in metazoans.[6]

HN1 has been implicated in promoting tumorigenesis for breast cancer,[7,8] liver cancer,[9–11] prostate cancer,[12] anaplastic thyroid cancer (ATC),[13] and cervical cancer.[14] HN1 protein in cytoplasm interacts with centrosome proteins and influences the bipolar spindle assembly in prostate cancer cells.[15] Its cell cycle-related function was recently shown where HN1 contributed to S-phase accumulation and cyclin B1 degradation via Cdh1 which is a cofactor of anaphase-promoting complex/cyclosome.[16] Furthermore, HN1 regulates the stemness of tumor growth in ATC to induce dedifferentiation. HN1 inhibited the CTCF expression and subsequent chromatin accessibility of differentiation genes.[17]

The SH-SY5Y cell line is a unique tool to study the differentiation of neuroblastoma cells to neuronal populations according to human cellular physiology.[18] Undifferentiated SH-SY5Y cells grow rapidly in clumps displaying short processes and remain depolarized.[19,20] Retinoic acid (RA)-differentiated SH-SY5Y cells, on the other hand, exhibit polarization, reduced proliferation, and extended or branched neurite outgrowth.[21,22] The SH-SY5Y cells in culture are classified as N-type showing neuron-like (neuroblastic) phenotype, and S-type as substrate or undifferentiated adherent phenotype.[21,23] Therefore, in this study, we utilized RA for differentiating SH-SY5Y cells,[21] developed neuron-like morphology to characterize the *HN1*-related differences in observed phenotypes. We used transcriptomics data analysis[24] to illustrate the expression levels of *HN1* in neuroblastoma, Parkinson's disease,[25] and RA-differentiated SH-SY5Y cells. Then, we explored the *HN1* coexpression network to understand the pathways enriched for genes coexpressing with *HN1* in neuroblastoma.[26] Finally, we performed in vitro experiments to understand the role of HN1 in undifferentiated SH-SY5Y cells and RA-differentiated neurons. The expression of HN1 was correlated with cell cycle-related proteins involved in either differentiation of SH-SY5Y cells or suppression of differentiation in RA-treated SH-SY5Y cells.

2 | MATERIALS AND METHODS

2.1 | Bioinformatics analysis of HN1

A violin plot was constructed based on comparison of *HN1* gene expression levels from the normal and tumor analysis ran on TNMPLOT[24] database where RNA-seq based data was queried. The platform option for the search was also based on pediatric tissues or non-cancerous patients. The neuroblastoma (TARGET) was selected as the data set. The microarray data from GEO data set GSE8397[27] with platform GPL96 was also searched for *HN1* mRNA levels to compare between normal and Parkinson's disease (PD) patients and the tissues were extracted from superior frontal gyrus (SFG), lateral substantia nigra (LSN), and medial substantia nigra (MSN) for both diseased and normal cases. The GSE9169 data set[28] obtained from the GEO database was analyzed using the GEO2R tool to evaluate the mRNA levels of *HN1*. The data contains RNA-seq analysis from control SH-SY5Y ($n = 3$) and RA-treated cells ($n = 3$) for different time periods. HN1 coexpressed genes were obtained from the c-bioportal database[26] with Spearman's coefficient cut-off at 0.5 from the TARGET-neuroblastoma data set. The gene list was then queried for Gene Ontology (GO) analysis using the Funrich v3.1.3 software package[29] and graphed according to −log10 and percentages of gene ratings provided within the visualization tool.

2.2 | Cell culture

The SH-SY5Y cell line was procured from the American Type Culture Collection and propagated in Dulbecco's modified Eagle medium (DMEM)-F12 medium. The cell-culture medium was supplemented with 10% fetal bovine serum (FBS) along with 1% L-glutamine, and 1% (100 U/mL) streptomycin/penicillin solution. The cells were grown in a humidified atmosphere containing 5% CO_2 in an incubator at 37°C. The passage number of the cells utilized in experimentation was kept under 15 BSL2 settings allowing contaminant-free cultures to propagate followed by routine standard mycoplasma testing in addition to 4′,6-diamidino-2-phenylindole (DAPI) staining in every passage when appropriate.

2.3 | Chemicals and antibodies

Thymidine (S-phase synchronizing agent), nocodazole (microtubule depolymerizing agent), taxol (microtubule polymerizing agent), SB216763 (GSK3β inhibitor), LY294002 (PI3K/AKT kinase inhibitor), and doxycycline (tetracycline analog) were obtained from Sigma-Aldrich. Anti-HN1 antibody was obtained from Invitrogen and an anti-β-actin antibody conjugated with horse-radish peroxidase (HRP) was obtained from Sigma-Aldrich. Anti-β-tubulin was obtained from Abcam. Antibodies against geminin, Cdt1, GSK3β, β-catenin, Akt, acetylated-α-tubulin, Cdk2, Skp2, GAP43, and GAPDH were obtained from Santa Cruz Biotechnology. A list of antibodies and their dilutions used in the study is given in Table 1.

2.4 | Transfections and stable HN1 or HN1-venus expressing SH-SY5Y cell line generation

2.4.1 | Cloning

HN1 overexpression in undifferentiated and RA-differentiated SH-SY5Y cells utilized HisMax-HN1

TABLE 1 List of antibodies and their dilutions used in the study.

Antibody	Technique	Manufacturer and catalog	Dilution
Anti-HN1	WB/IF	Invitrogen—PA5-109824	1/750–1/200
Anti-BrdU	IF	Abcam (ab142567)	1/200
Anti-β-actin	WB	(HRP) conjugated	1/500.000
Anti-geminin	WB	Invitrogen—PA5-38612	1/1000
Anti-GSK3ß	WB	Santa Cruz—sc377213	1/600
Anti-β-catenin	WB	Santa Cruz—sc59737	1/500
Anti-Akt	WB	Cell Signaling—9272 C5	1/1000
Anti-β-tubulin	WB/IF	Abm—G098	1/10.000–1/300
Anti-∝-ac-tubulin	WB	Santa Cruz—sc23950	1/600
Anti-Cdt1	WB	Santa Cruz—sc365305	1/1000
Anti-GAPDH	WB	Ambion—AM4300	1/100.000
Anti-p-GSK3ß(Ser21)	WB	Santa Cruz—sc130601	1/500
Anti-Cdk2	WB	Santa Cruz—sc6248	1/500
Anti-Skp2	WB	Santa Cruz—sc74477	1/600
Anti-GAP43	WB	Santa Cruz—sc17790	1/1000
Anti-lamin B1	WB	Santa Cruz—sc365962	1/600
Anti-Rabbit-HRP conjugated	WB	Sigma	1/20.000
Anti-Mouse-HRP conjugated	WB	Sigma	1/30.000
Alexa488/532/594 (anti-mouse IgG)	IF	Millipore	1/600
Alexa488/532/594 (anti-rabbit IgG)	IF	Millipore	1/600

Abbreviations: HRP, horse-radish peroxidase; IF, immunofluorescence; IG, immunoglobulin G; WB, Western blotting.

plasmid containing HN1 ORF cloned into the plasmid backbone of pcDNA4-HisMax and used in the prior study as well.[15] FUGENE HD reagents obtained from Promega (Cat. No. E2311) were used for plasmid DNA transfection. Briefly, cells were seeded in 6-cm cell-culture dishes and after 1 day, 1 μg DNA and 3 μL transfection reagent mixture in 100 μL full negative DMEM F-12 media was incubated for 15 min and added to the cell-culture dish containing a monolayer of cells. After completion of the treatment period (48 h), cells were harvested by scraping the monolayer using a cell scraper and centrifuged to precipitate cells with phosphate buffer saline (PBS) (pH 7.4). The cells were processed further for protein isolation. pcDNA4-HisMax without gene of interest was used as mock control (HM-Vector) and HM-HN1 was used for ectopically expressing HN1.

2.4.2 | Transfections for lentivirus production

The pcDNA4-TO-Venus plasmid was used to clone *HN1* with or w/o Venus, and then the insert fragments were cloned into pCW57.1 backbone to construct an all-in-one inducible expression system expressing *HN1* and/or *HN1*-Venus as described previously.[16] pCW57.1-HN1 and pCW57.1-HN1-Venus plasmids were then used as transfer vectors together with packaging plasmids such as pMD2G, pRSV-Rev, and PMDLg/pRRE for transfection into HEK293T cells. Polyethyleneimine was used as a transfection reagent with a ratio of 1:3 (DNA: transfection reagent). To boost up the transfection efficiency 25 μM chloroquine (Sigma-Aldrich) was used before transfection. Viral particles in the culture media were collected from HEK293T supernatant derived after centrifugation (300 g for 10 min) and filtering posttransfection (48–72 h). Lentiviral particles were concentrated via centrifugation at 16 000*g* for o/n, resuspended in PBS, aliquoted, and stored at −80°C until use.

2.4.3 | Transductions and stable cell generation

The lentivirus transduction protocol involved polybrene (Sigma-Aldrich) as the transduction reagent (10 μg/mL). The transduction period was 72 h. Then the culture medium was replaced with fresh media to kept for 24 h, then puromycin (Sigma-Aldrich) (1 μg/mL) was added to the cells in culture. The cells were kept in puromycin-containing media for 6–10 days to obtain stable SH-SY5Y cells inducible for *HN1* and *HN1*-Venus expressions. Doxycycline inductions were performed at the time of use for the cells with or w/o treatments.

2.5 | Protein isolation, separation, and immunoblotting

Radio-immunoprecipitation assay (RIPA) buffer (ice-cold) was employed for lysing cells as described in our previous study. The final RIPA buffer used for the cell lysis contains 1 mM Na_3VO_4, 1 mM ethylenediaminetetraacetic acid (EDTA), 1 mM NaF, 150 mM NaCl, 0.25% Na-deoxycholate, 50 mM Tris-HCl (pH 7.4), and 1% Nonidet P-40, supplemented with Phospho-Stop and protease inhibitors (Roche). The cellular pellets mixed with RIPA buffer were placed on ice for 45 min before sonication for 50 cycles, with 25% power for 20 s for complete homogenization. After sonication, the lysates were centrifuged at 12 000*g* for 10 min at 4°C, and the supernatant was collected as the total protein lysate. The protein concentration was determined using a BCA Assay Kit (Sigma-Aldrich), according to the manufacturer's recommendation.

The collected protein lysates (50 μg/sample) were separated using sodium dodecyl-sulfate-polyacrylamide (10%–15%) gels with electrophoresis. The wet transfer method was applied for transferring proteins to the polyvinylidene difluoride (PVDF) membrane. The immobilized proteins on the membrane were then blocked with 5% milk solution prepared in 0.1% Tween-20 in Tris-buffered saline (TBS-T) for 1 h, followed by incubation with primary antibodies (1 h at room temperature or overnight at 4°C). The primary antibodies were then washed with TBS-T solution for half an hour and replaced with a secondary antibody conjugated with HRP, which was also washed subsequently. For chemiluminescence, an enhanced chemiluminescence reagent obtained from BioRad was used on the PVDF membrane and the resulting light was captured on X-ray film exposed on the membrane (kept between plastic sheets) in the dark room and developed using conventional developer and fixer solutions. Immunoblots are normalized based on β-actin or GAPDH levels where indicated and independent repeats are shown in Supporting Information.

2.6 | Immunofluorescence imaging

To capture immunofluorescent proteins in SH-SY5Y cells, cells were grown on sterile cover slips in either 35 mm culture dishes or six-well plates. After completing the treatments, cells were fixed with either

paraformaldehyde (4% in PBS) at room temperature or ice-cold methanol (100%) at −20°C for half an hour. After fixation, cells were permeabilized using 0.2% Triton-X solution in PBS for 5 min, followed by blocking in 1% bovine serum albumin solution in PBS for 5 min on a shaker at room temperature. After blocking, cells were subjected to incubation with primary antibodies at 37°C for 1 h. Unbound antibodies were washed with PBS and Alexa-fluor conjugated secondary antibodies were used according to the host of primary antibodies. After antibody labeling, cells were washed with PBS and kept in 70% ethanol and 100% ethanol solutions for dehydration. After air drying the cover glasses, DAPI (1 μg/mL) in 30% glycerol solution in PBS was used to mount for visualization of nuclei. Glass slides were kept in the dark for 15 min and the images were captured using DM4000 LED B Leica fluorescence microscope equipped with 5.5. Megapixel digital camera and Leica Application Suite software (LAS v4.4.0). At least eight images were taken from each sample ($n = 3$) containing more than 10 cells per field to compare the cellular populations depending on the experiment.

2.7 | Cell cycle distribution analysis

Cells after treatments were trypsinized and washed with PBS and fixed with 70% ethanol at least overnight at −20°C. After fixation, cells were washed with PBS using centrifugation procedures, permeabilized with 0.2% Triton-X-100 in PBS, and subsequently treated with RNAse A (20 μg/mL) in PBS. After centrifugation, cells were suspended in propidium iodide solution (5 μg/mL) in PBS and placed in the dark at room temperature for 15 min. DNA content analysis was then performed using an Accuri C6 flow cytometer (Becton Dickinson) and Flowjo (v10) software. The final gated population with threshold of $1–2 \times 10^4$ cells was selected for comparing the samples.

2.8 | Subcellular fractionation

Briefly, cells after treatments were washed with PBS and centrifuged for pelleting cells and suspended in Buffer A containing 1 mM ethylene glycol-bis(β-aminoethyl ether)-N,N,N′,N′-tetraacetic acid (EGTA), 1 mM EDTA, 50 mM 4-(2-hydroxyethyl)-1-piperazineethanesulfonic acid (HEPES) (pH 7.4), and 10 mM KCl and placed on a rotator for 30 min at 4°C. Cytoplasmic fraction was collected from the supernatant after centrifugation at 4000*g* for 5 min at 4°C. The pellet was washed in Buffer A four times for the removal of the cytoplasmic fraction. After washings, pellets were suspended in Buffer B containing 0.5% Triton-X-100, 1 mM EGTA, 1 mM EDTA, 1 M HEPES (pH 7.4), and 400 mM KCl and shaken on a rotator for 30 min at 4°C. After shaking, supernatant from the centrifugation at 14 000*g* for 30 min at 4°C, was collected as the nuclear fraction. The nuclear and cytoplasmic fractions were quantified for protein concentration as described for total protein lysates before. Anti-GAPDH was used to determine cytoplasmic fractionation, and anti-Lamin B1 was used as the loading control for nuclear lysates.

2.9 | Statistical analysis

The data graphed in bar or line graphs are taken as the means ± standard error of the mean for independent setups for the analyses and shown in either main figures or Supporting Information data files. For visualization, Microsoft Excel or GraphPad Prism 9 software packages were used. Where applicable, the differences in variances are recorded according to *p*-value (<0.05) based on analysis of variance (ANOVA), two ways ANOVA or multiple unpaired *t* test to show the statistical significance (*).

3 | RESULTS

3.1 | HN1 is upregulated in neuroblastoma, downregulated in RA-differentiated neurons, and fluctuates during cell cycle

The transcriptomics data set available in the TNMPLOT database for the normal and tumor analysis was used to compare the HN1 expression levels.[24] The neuroblastoma (TARGET) was selected as the data set. The Mann–Whitney *p*-value for HN1 level comparison between normal and cancer tissues was recorded as 1.15^{e-55} and fold change mean as 10.13 and the fold change median as 10.89 from 190 normal samples and 149 tumor samples (Figure 1A). Therefore, *HN1* transcript levels are significantly higher in neuroblastoma as compared to normal controls indicating that *HN1* may act as a tumor-promoting gene. *HN1* mRNA levels in SFG, LSN, and MSN tissues from normal and Parkinson's disease patients were compared using the GEO2R tool on the GSE8397 data set. The data were originally obtained from the tissues of normal and PD patients from SFG ($n = 3$ normal, $n = 4$ PD), LSN ($n = 4$ normal, $n = 7$ PD), and MSN ($n = 7$ normal, $n = 7$ PD) for both diseased and normal cases. HN1 levels were found to be lower in PD as

compared to normal counterparts (Figure 1B). The neurodegenerative disease exhibited lower HN1 levels, whereas tumorigenic neuroblastoma manifested higher HN1 levels, thereby indicating that HN1 has a role in cellular growth in neuronal populations.

Another GEO data set containing data from the SH-SY5Y cells treated with RA for up to 5 days was queried for *HN1* mRNA levels. *HN1* levels gradually decreased upon exposure of SH-SY5Y cells to RA, which is routinely used for differentiating neuroblastoma cells to neurons (Figure 1C). The Kruskal–Wallis's test utilizing nonparametric or mixed analysis of ANOVA was used for statistical analysis, where $p = 0.0355$ indicated a significant difference of *HN1* decrease. The *HN1* coexpressed genes were extracted from neuroblastoma (TARGET) data set and used as input for generating the GO terms for biological pathways. It was observed that the most enriched and statistically significant (File S1) pathways are DNA replication, nuclear mRNA splicing, DNA repair, mitotic cell cycle, chromatin organization, and cell division (Figure 1D). Therefore, it is assumed through bioinformatics analysis that *HN1* is upregulated in neuroblastoma, downregulated in PD and RA-differentiated neurons and its coexpressed genes function in the regulation of the cell cycle.

SH-SY5Y cells were differentiated into neuron-like cells through induction via RA as reported previously[30] and we also have observed using phase contrast microscopy in SH-SY5Y cell culture (Figure 2A). Furthermore, when HN1 protein levels were measured after continuous treatment of SH-SY5Y cells with RA, it was observed that HN1 expression level gradually decreased upon exposure to RA (Figure 2B). Therefore, *HN1* mRNA (Figure 1C) and protein expressions (Figure 2B) decrease upon differentiation of neuroblastoma cells to neuron-like cells (three independent repeats; Figure S1) and statistical analysis for two-way ANOVA are shown in File S2; Figure S2). Since the HN1 coexpression network is enriched for cell-cycle-related pathways, we employed

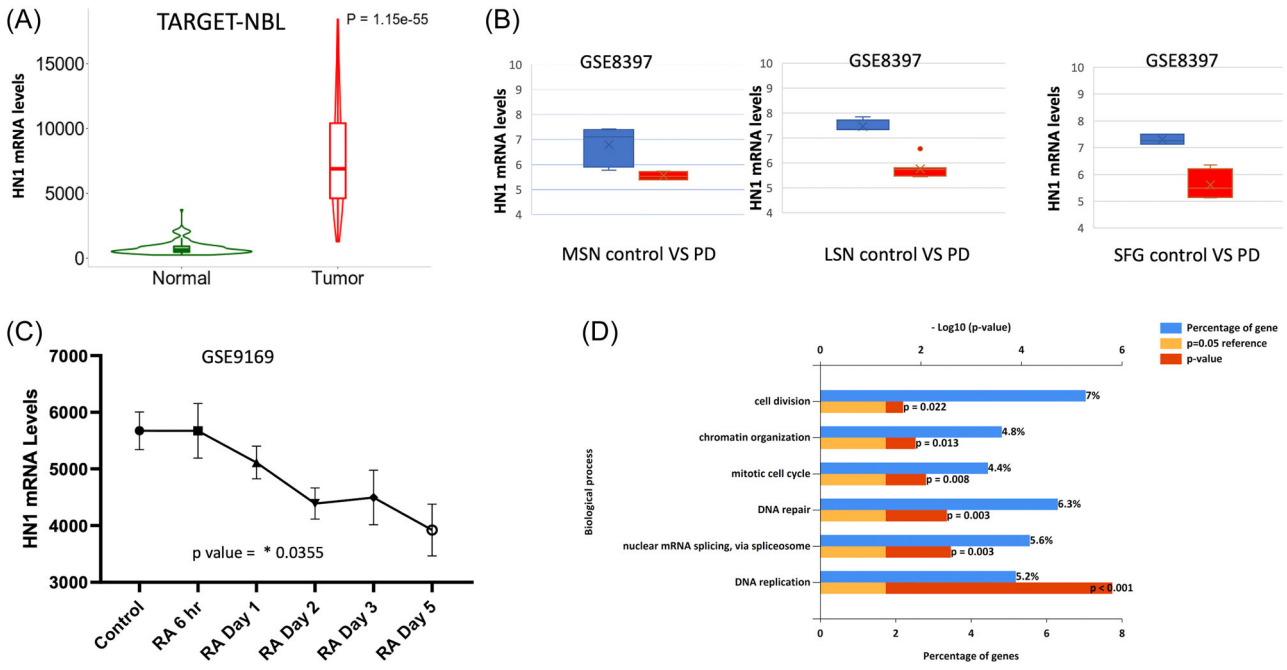

FIGURE 1 HN1 levels from transcriptomics data and pathways enriched in its coexpression network. (A) A violin plot was constructed based on comparison of HN1 gene expression levels from the normal and tumor analysis ran on TNMPLOT database where RNA-seq based data was queried from TARGET-NBL datasets. The platform option for the search was also based on pediatric tissues or noncancerous patients. The neuroblastoma (TARGET) was selected as the data set. (B) The microarray data from GEO data set GSE8397 with platform GPL96 was also searched for *HN1* mRNA levels to compare between normal and PD patients and the tissues were extracted from SFG ($n = 3$ normal, $n = 4$ PD), LSN ($n = 4$ normal, $n = 7$ PD), and MSN ($n = 7$ normal, $n = 7$ PD) for both diseased and normal cases. The box plots are drawn in Microsoft Excel. (C) The RNA-seq data from GSE9169 GEO data set was queried for *HN1* mRNA levels and plotted using GraphPad Prism 9, where $n = 3$ for each sample of SH-SY5Y cells treated with RA for indicated periods ($p = 0.0355$, * for nonparametric Kruskal–Wallis test). (D) *HN1* coexpressed genes (290) with Spearman's coefficient more than 0.5 with $p < 0.05$, were extracted from TARGET-neuroblastoma data set using c-Bioportal and subjected to Gene Ontology analysis for biological pathways using Funrich v3.1 software package. The statistically relevant enriched pathways are shown in the graph. LSN, lateral substantia nigra; mRNA, messenger RNA; MSN, medial substantia nigra; PD, Parkinson's disease; RA, retinoic acid; SFG, superior frontal gyrus.

cell-cycle synchronization approaches to determine phase-specific protein levels of HN1 in SH-SY5Y cells. HN1 protein levels are enriched only in the S-phase represented by the samples with double thymidine block and release (Figure 2C), consistent with our previous studies. Moreover, the experiment was repeated with longer releases from double thymidine blocks, and HN1 levels remained enriched in S-phase of the cell cycle (Figure 2D). Furthermore, the cells were released from the nocodazole block (post-G2) to G1 for up to 10 h, and HN1 levels remained lower than control cells (Figure 2E). Since serum starvation leads to G0/G1-enrichment and HN1 levels were lower in the G1 phase, a serum-gradient experiment was conducted to observe the effect of change growth parameter (serum) in SH-SY5Y cells. HN1 levels increased upon the addition of FBS into cell-culture media (Figure 2F). Therefore, HN1 being downregulated in RA-differentiated cells and serum starvation along with its upregulation upon addition of FBS and in the S-phase of the cell cycle indicates that HN1 is involved in the proliferation of neurons or likely in their dedifferentiation.

3.2 | HN1 overexpression alters cell cycle dynamics in undifferentiated and RA-differentiated SH-SY5Y cells

HN1 overexpression using plasmid DNA transfection was carried out in undifferentiated and RA-differentiated SH-SY5Y cells. HN1 overexpression increased geminin levels in undifferentiated cells (Figure 3A) but not

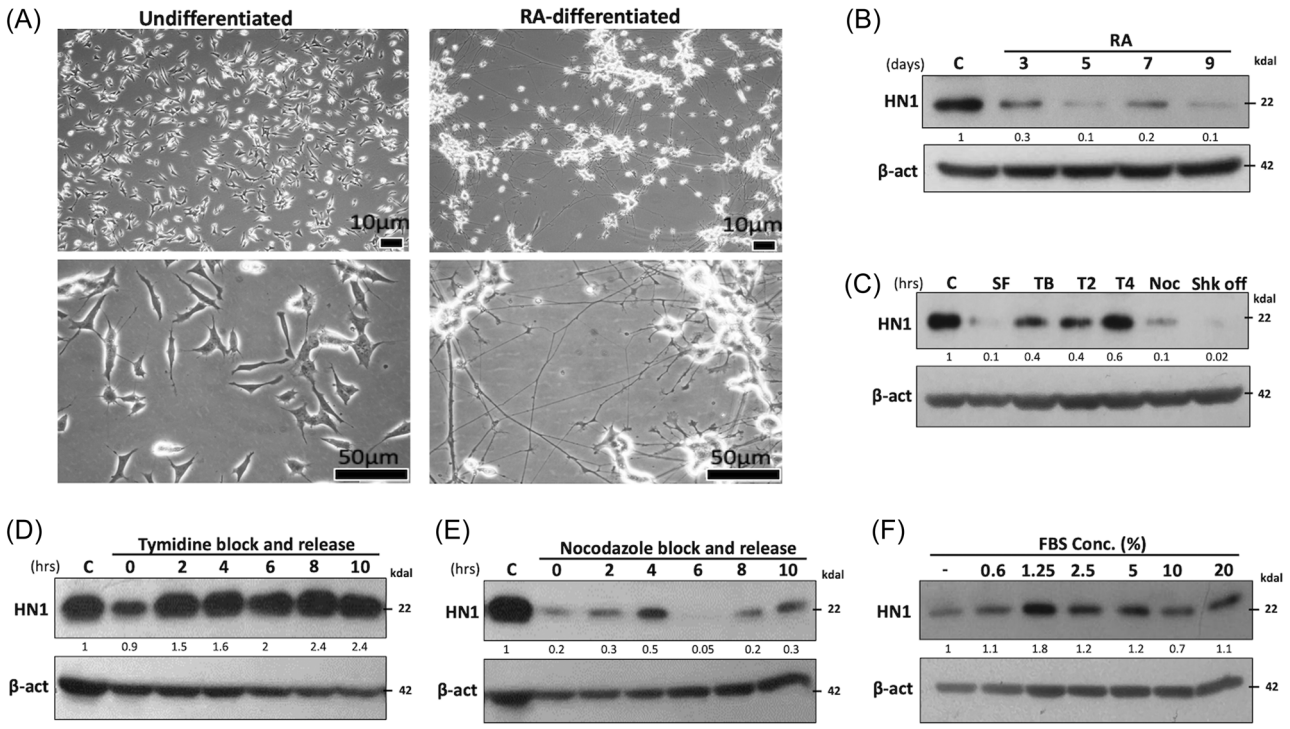

FIGURE 2 HN1 expression level decreases upon differentiation of SH-SY5Y cells and is enriched in S-phase of the cell cycle. (A) The SH-SY5Y cells were subjected to all-trans RA treatment (10 µM) for 2 weeks and photographed in an inverted phase contrast microscope. The neurite growth is clearly visible in RA-treated differentiated cells on the right side of the panel (upper ×10 and lower ×40 images). (B) Cells treated with RA for up to 9 days were collected, lysed, and isolated protein lysates were immunoblotted with anti-HN1 and anti-β-actin antibodies. The data for three independent repeats and relevant two-way ANOVA is available in Supporting Information. The difference between undifferentiated versus RA-differentiated samples is statistically significant $p < 0.001$. (C) Cells were synchronized in different phases of the cell cycle using different approaches to get enriched populations for G1 (serum-free), G1/S (double thymidine block), early S (double thymidine block and release into S for 2 h), S (middle) (4 h release from double thymidine block), post-G2 (nocodazole block), and M (mitotic shake-off after release from nocodazole block for 1 h and collecting suspended cells). Protein lysates were immunoblotted with anti-HN1 and anti-β-actin bodies. (D) The cells were released from indicated time periods from double thymidine blocks and subjected to immunoblotting with anti-HN1 and anti-β-actin antibodies. (E) The cells were released from nocodazole block for indicated periods and immunoblotting was performed using anti-HN1 and anti-β-actin antibodies. (F) The cells were cultured in normal culture media with increasing concentrations of FBS for 48 h and immunoblotted with anti-HN1 and anti-β-actin antibodies (immunoblot in [B] was repeated three times for HN1 quantitation). ANOVA, analysis of variance; FBS, fetal bovine serum; RA, retinoic acid.

changed in RA-differentiated cells, which is also consistent with the cell cycle distribution assay showing increased S and G2 populations (Figure 3B,D). Upon HN1 overexpression, GSK3β levels also increased in undifferentiated SH-SY5Y. However, in RA-differentiated cells, GSK3β levels remained unchanged (from two independent experiments shown in File S2; Figure S3). Since inhibition of GSK3β is implicated in preventing RA-mediated differentiation of SH-SY5Y cells,[31] HN1 overexpression bearing no change in differentiated cells for GSK3β and increasing it in undifferentiated cells indicates that HN1 acts differently in RA-differentiated cells. HN1 overexpression also increased β-catenin levels in both conditions,

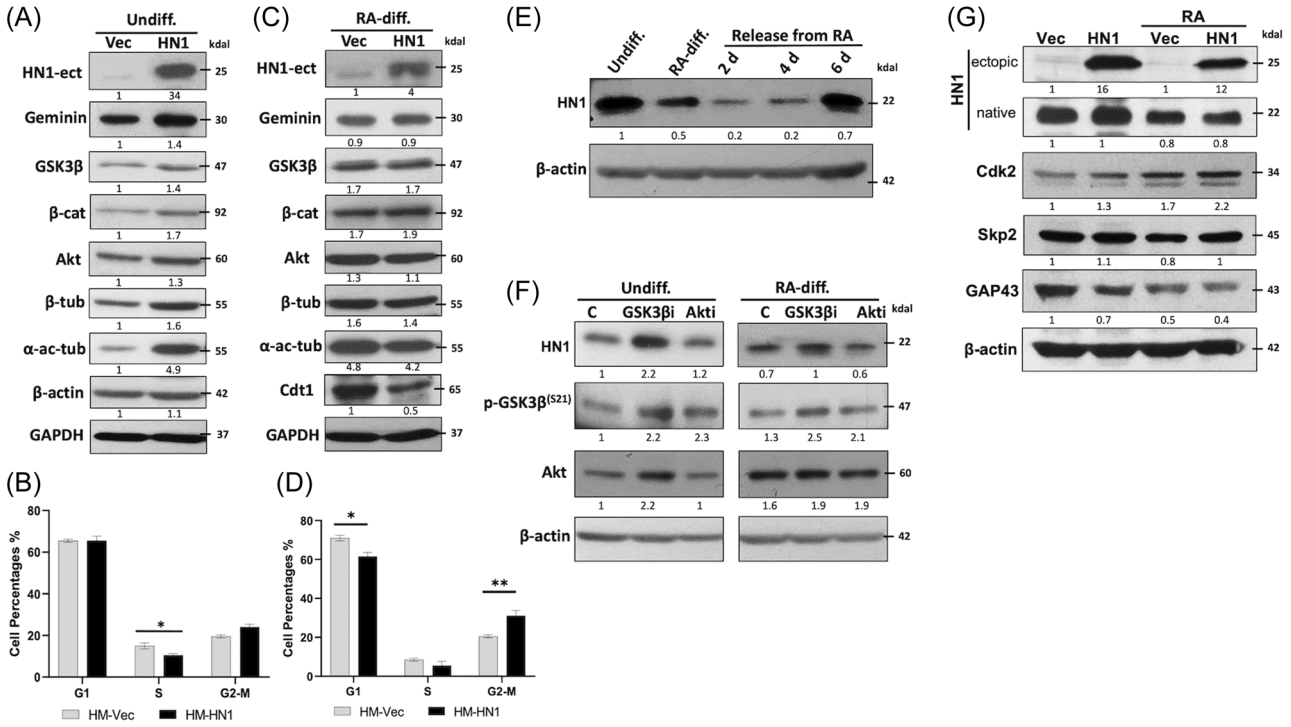

FIGURE 3 The effect of HN1 overexpression on undifferentiated and RA-differentiated SH-SY5Y cells. (A) Undifferentiated SH-SY5Y cells were transfected with either HM-Vec or HM-HN1 plasmids and immunoblotting was performed on protein lysates collected at 48 h posttransfection. Antibodies against HN1, geminin, β-catenin, GSK3β, Akt, β-tubulin, acetyl-α-tubulin, β-actin, and GAPDH were used for WB analysis. (B) The cells (10%) from (A) were fixed and stained with PI before flow cytometry. The FlowJo v10 software was used for analyzing cell population percentages in G1, S, and G2 (also M) are plotted (mean values), where gray bars represent HM-Vector and black bars represent HM-HN1 sample. Multiple unpaired *t* test was performed on flow cytometry data and statistically significant different samples are highlighted with * sign. (C) RA-differentiated SH-SY5Y cells were transfected with either HM-Vector or HM-HN1 plasmids and immunoblotting was performed on protein lysates collected at 48 h posttransfection. Antibodies against HN1, geminin, Cdt1, β-catenin, GSK3β, Akt, β-tubulin, acetyl-α-tubulin, and GAPDH were used for WB analysis. Graphical representation was given as histogram, where the fold change for each protein expression was calculated as RA/undiff w/wo HN1 expression. Two independent repeats for WB for (A) and (C) for HN1, GSK3β, and α-acetyl-tubulin are shown in Supporting Information. (D) The cells (10%) from (C) were fixed and stained with PI before flow cytometry. The FlowJo v10 software was used for analyzing cell population percentages in G1, S, and G2 (also M) are plotted (mean values), where gray bars represent HM-Vector and black bars represent HM-HN1 sample. Multiple unpaired *t* test was performed on flow cytometry data and statistically significant different samples are highlighted with * sign. (E) The effect of removal of RA from RA-differentiated cells was measured by first differentiating SH-SY5Y cells with RA treatment (10 μM) for 2 weeks and then RA was removed from cell-culture media for indicated periods (2, 4, and 6 days) and immunoblotting was performed with anti-HN1 and anti-β-actin antibodies. (F) The effects of the GSK3β and Akt inhibitions were measured in undifferentiated and RA-differentiated SH-SY5Y cells. Total of 10 μM SB216763 (GSK3-β inhibitor) and 25 μM LY294002 (PI3K/Akt kinase inhibitor) were used, and exposure of the inhibitors was 6 h. For WB analysis anti-HN1, anti-pGSK3β$^{(Ser21)}$, anti-β-Akt, and anti-β-actin were used. The independent repeats and histograms and related two-way ANOVA analysis are shown in the Supporting Information data. The difference between undifferentiated versus RA-differentiated samples is statistically significant $p < 0.05$. (G) Undifferentiated and RA-differentiated SH-SY5Y cells were transfected with either HM-Vec or HM-HN1 plasmids and immunoblotting was performed on protein lysates collected at 48 h posttransfection. Antibodies against HN1, Cdk2, Skp2, GAP43 and β-actin were used for WB analysis. All blots were normalized to β-actin. ANOVA, analysis of variance; FBS, fetal bovine serum; PI, propidium iodide; RA, retinoic acid; WB, western blot.

demonstrating that HN1 is involved in regulating β-catenin related events (Figure 3A,C), likely influencing the transcriptional profiling for the differentiation. Furthermore, the β-catenin level remains stable upon RA-differentiation in controls w/o HN1 overexpression,[32] its upregulation is associated with neuronal differentiation and survival.[33] Therefore, cells stabilized for HN1 demonstrating upregulated β-catenin levels, implying that HN1 increases the survival phenotype of both undifferentiated and RA-differentiated SH-SY5Y cells. The Akt levels also increased in undifferentiated cells (Figure 3A) and decreased in RA-differentiated cells (Figure 3C) when HN1 was overexpressed. The Akt upregulation has been regarded as an indication of differentiation of SH-SY5Y cells,[34,35] therefore, Akt decrease in RA-differentiated cells indicates that HN1 acts as a dedifferentiating factor in SH-SY5Y cells. Furthermore, HN1 overexpression stabilized cytoskeletal factors such as β-tubulin and α-acetylated-tubulin (from two independent experiments shown in File S2; Figure S3) in undifferentiated SH-SY5Y cells, which are downregulated in RA-differentiated cells.

The cells released from RA for up to 6 days after differentiation exhibit a significant stabilization of HN1, implying that RA suppresses HN1 in SH-SY5Y cells (Figure 3E). Since GSK3β activity is required for the differentiation of SH-SY5Y cells,[31] the effect of GSK3β inhibition using its inhibitor was evaluated in undifferentiated and RA-differentiated SH-SY5Y cells. GSK3β inhibition stabilized HN1 protein levels in both cases, implying that HN1 downregulation during RA-differentiation could be due to GSK3β signaling (Figure 3F) (at least from two independent experiments shown in File S2; Figure S4). It has already been established that GSK3β is an upstream kinase of HN1[16] (Figure S5). Moreover, RA-differentiation induces PI3K/Akt signaling as well,[34] however, the inhibition of this pathway using LY294002 did not alter HN1 levels in undifferentiated SH-SY5Y cells, but reduced HN1 levels in RA-differentiated cells (Figures 3F and S5), further suggesting that HN1 is a dedifferentiating factor in neuroblastoma cells (from two independent experiments shown in File S2; Figure S3).

To reveal the direct impact of HN1 overexpression on mature neuronal marker (GAP43),[36] we repeated our experiment and performed western blot analysis to show that HN1 overexpression upon plasmid transfection reduces the expression of GAP43 in both undifferentiated and RA-differentiated SH-SY5Y cells (Figure 3G). Conversely, Cdk2 expression indicating the progression of cell cycle, was increased in HN1 overexpressed samples, implying that HN1 functions in promoting the growth of SH-SY5Y cells and in RA-treated cells, therefore, it leads to the progression of cell cycle which is linked with dedifferentiation of neuronal populations.[37] Moreover, Skp2 degradation has been linked with neuronal differentiation with RA-treatment,[38] here we showed that HN1 overexpression in both undifferentiated and RA-differentiated SH-SY5Y cells, Skp2 is accumulated as compared to control cells. This line of evidence further strengthens our hypothesis that HN1 is involved in regulating dedifferentiation of SH-SY5Y cells.

3.3 | Microtubule dynamics control HN1 levels in undifferentiated and RA-differentiated SH-SY5Y cells

Microtubule outgrowth in neurites due to the differentiation process is prominent in SH-SY5Y cells.[39] We investigated the microtubule polymerization and de-polymerization effect of HN1 expression in undifferentiated and RA-differentiated SH-SY5Y cells. We observed that RA-differentiated cells have depleted HN1 staining in comparison to undifferentiated SH-SY5Y cells (Figure 4A). Furthermore, the Nocodazole treatment led to the destabilization of HN1 and β-tubulin expression levels, whereas using taxol increased HN1 expression, distribution, and microtubule polymerization (Figure 4A–C). The immunoblotting with the same experimental design showed that in undifferentiated SH-SY5Y cells, HN1 levels correlated with β-tubulin upon using nocodazole (Figure 4B) and taxol (Figure 4C) (from three independent experiments shown in File S2; Figures S6 and S7). However, in RA-differentiated cells, HN1 levels increased slightly upon nocodazole treatment, which depolymerizes microtubules, further showing that in differentiated neurons, microtubule depolymerization stabilizes HN1, whereas taxol treatment also increased HN1 as well as tubulin in RA-differentiated cells. Thus, HN1 expression level or stability correlates with microtubule dynamics in SH-SY5Y cells.

3.4 | HN1 is a dedifferentiation factor involved in promoting the cell cycle in neuroblastoma cells

Since HN1 has been implicated in cell cycle regulation,[15,16] the temporal response of HN1 manipulation can give insights into its function, therefore HN1 inducible expression system was established. The effect of inducible HN1 expression on N- and S-type populations of SH-SY5Y cells was measured. HN1 overexpression demonstrated with HN1-Venus expression showed an increase in S-type populations of SH-SY5Y cells as compared to Venus-expressing cells (Figure 5A,B). The

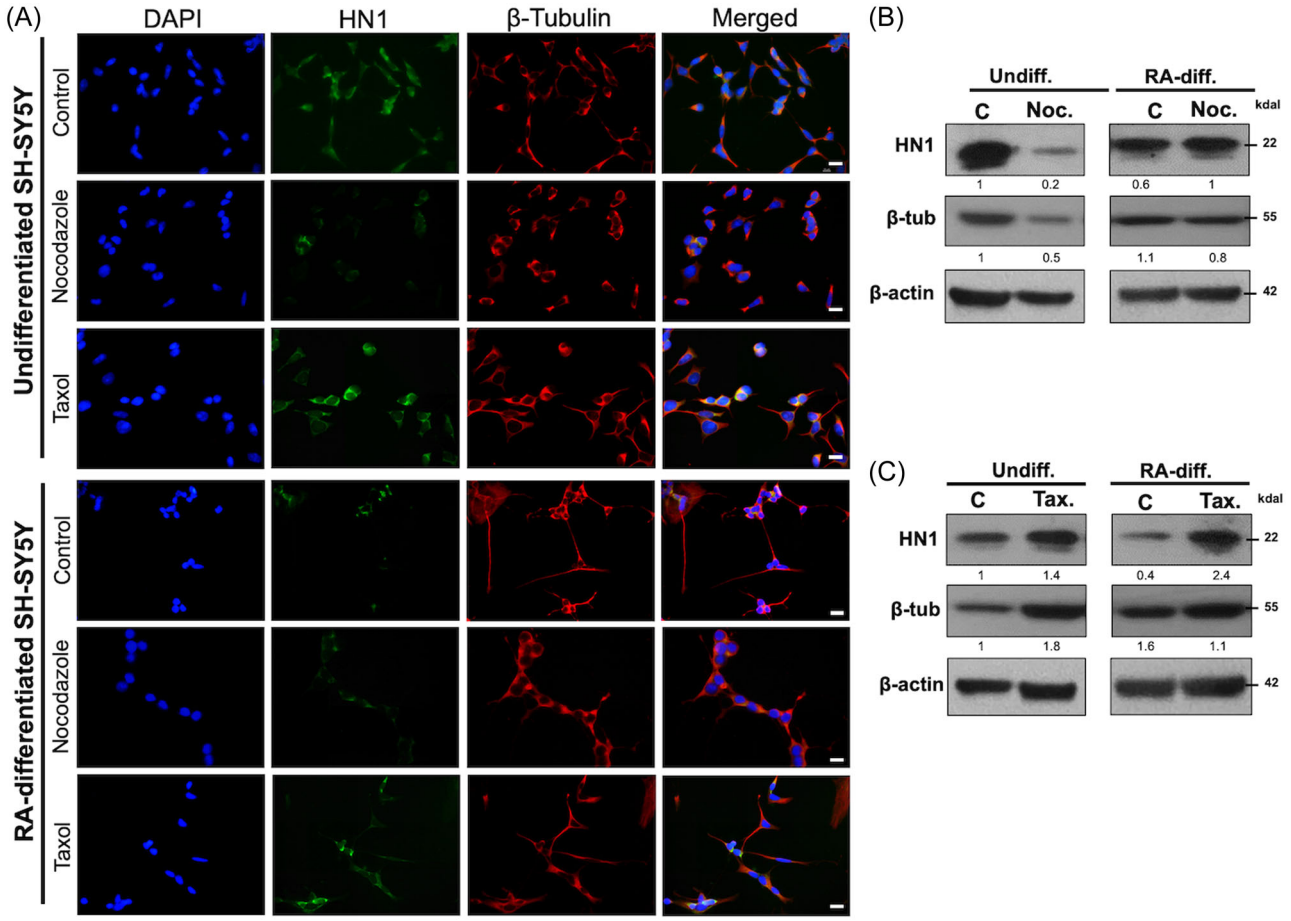

FIGURE 4 HN1 levels are correlated with microtubule dynamics in SH-SY5Y cells. (A) Undifferentiated and RA-differentiated SH-SY5Y cells grown on cover slips were treated with nocodazole (165 nM) or taxol (5 nM) for 1 h and fixed with methanol and processed for immunofluorescence microscopy. HN1 was labeled with anti-Alexa Fluor-488 (green) secondary antibody and β-tubulin was stained with anti-Alexa Fluor-594. DAPI was used for nuclear staining. Scale bar representing 10 μm is shown. (B) Undifferentiated and RA-differentiated SH-SY5Y cells treated with nocodazole (165 nM) for 1 h were processed for immunoblotting with anti-HN1, anti-β-tubulin and anti-β-actin antibodies. (C) Undifferentiated and RA-differentiated SH-SY5Y cells treated with taxol (5 nM) for 1 h were processed for immunoblotting with anti-HN1, anti-β-tubulin, and anti-β-actin antibodies. The (B) and (C) experiments were repeated three times, WB and associated statistical two-way ANOVA analysis is shown in Supporting Information. The difference between undifferentiated versus RA-differentiated samples is statistically significant $p < 0.001$ for nocodazole whereas not for taxol treatment $p > 0.05$. ANOVA, analysis of variance; DAPI, 4′,6-diamidino-2-phenylindole; RA, retinoic acid; WB, western blot.

N-type and S-type distribution parameters have been explained previously.[40] The enrichment of S-type cells in HN1 overexpressed cells demonstrates that HN1 expression is linked with the dedifferentiation of SH-SY5Y cells. In the HN1-Venus sample, the G2-M phase of the cell cycle increased significantly (Figure 5C), which is consistent with the previous data (Figure 3).

The effect of HN1 overexpression on nuclear accumulation of β-catenin and geminin was measured using fractionation of cellular lysates after plasmid transfection in both undifferentiated (RA−) and RA-differentiated (RA+) SH-SY5Y cells (Figure 5D). HN1 increased the nuclear accumulation of β-catenin in both undifferentiated and RA-differentiated cells. Nuclear accumulation of β-catenin has been demonstrated as a factor of dedifferentiation of RA-differentiated SH-SY5Y cells upon GSK3β inhibition.[31] Therefore, HN1 overexpression leads to a similar phenotype and increase in the S-type population, further strengthening the hypothesis that HN1 is a dedifferentiating factor.

HN1 overexpression stabilized geminin levels more prominently in undifferentiated cells (Figure 5D) in the nucleus, showing a G2-phase increase as it was shown previously. Concurrently, stable expression of HN1 in HN1-Venus expressing cells led to a significant increase in BrdU accumulation (Figure 5E,F), showing that HN1 overexpression increases the replicative and/or

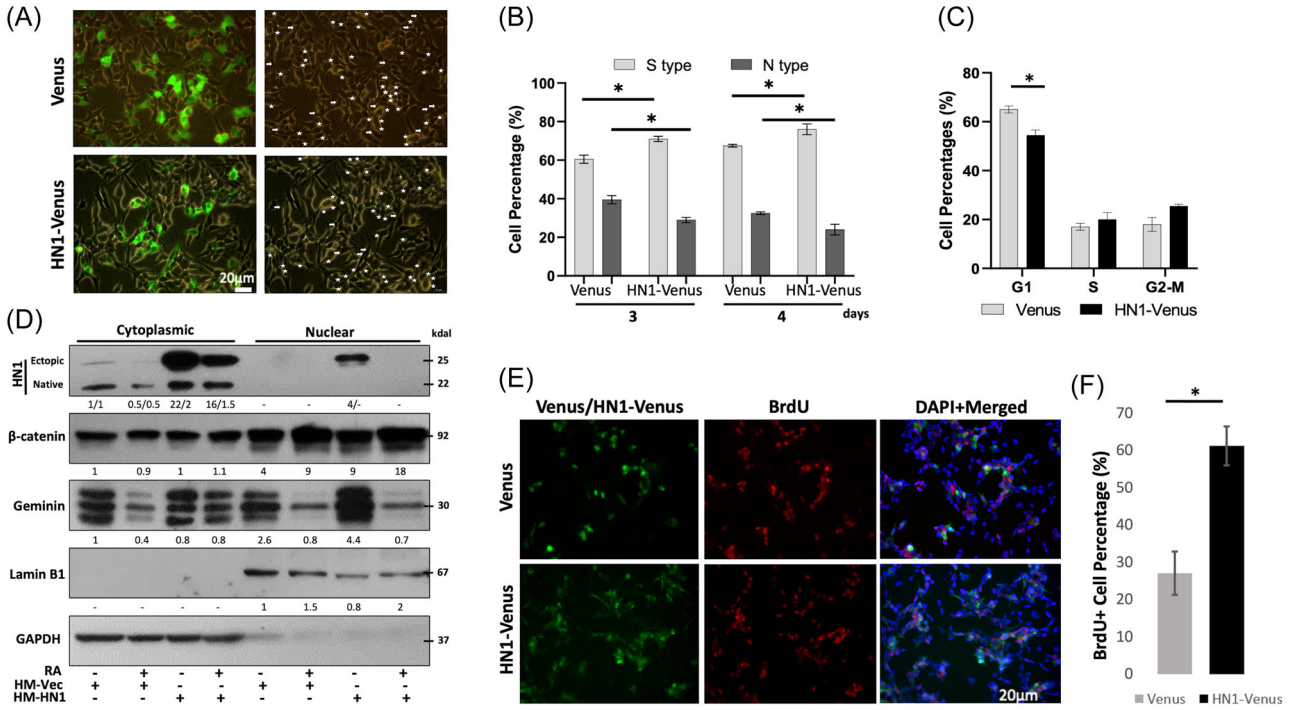

FIGURE 5 HN1 overexpression increases S-type SH-SY5Y cells, accumulates b-catenin in nucleus, and augments BrdU incorporation. (A) The SH-SY5Y cells stabilized with pCW57.1-Venus and pCW57.1-HN1-Venus viral particles were subjected to doxycycline (0.5 μg/mL) treatment for 3 days and photographed under an inverted fluorescence microscope. The individual cells positive for Venus and HN1-Venus are marked with arrows and stars, where arrows represent N-type and stars represent S-type SH-SY5Y cells. (B) The statistical data was plotted to compare the number of N-type and S-type cells in Venus and HN1-Venus expressing cells for both 3 and 4 days of doxycycline treatments. The two-way ANOVA test was performed, and statistically significant groups of matched samples are shown with * sign. (C) The pCW57.1-Venus and pCW57.1-HN1-Venus cells treated with doxycycline (0.5 μg/mL) were fixed with ethanol and stained with PI and analyzed for DNA content analysis. The graph represents the mean number of G1, S, and G2/M populations in Venus and HN1-Venus expressing SH-SY5Y cells. (D) The effect of HN1 overexpression on nuclear-cytoplasmic localization of different proteins was measured in undifferentiated and RA-differentiated SH-SY5Y cells by transfecting HM-Vector and HM-HN1 plasmids. The cytoplasmic and nuclear fractions were immunoblotted with antibodies against HN1, β-catenin, geminin, lamin B1, and GAPDH. (E) The pCW57.1-Venus and pCW57.1-HN1-Venus cells treated with doxycycline (0.5 μg/mL) for 3 days. One hour before cells were fixed with paraformaldehyde and methanol subsequently, cells were treated with BrdU. After fixation, cells were probed with anti-BrdU primary antibody and then secondary Alexa-594 (mouse). DAPI was used to stain nuclei. (F) The BrdU-positive Venus and HN1-Venus expressing cells were counted ($n = 3$) and mean BrdU-positive cell percentages were graphed. ANOVA, analysis of variance; DAPI, 4′,6-diamidino-2-phenylindole; PI, propidium iodide; RA, retinoic acid; WB, western blot.

proliferative SH-SY5Y cells, thus promotes the de-differentiation of neuroblastoma cells, perhaps more in S type.

4 | DISCUSSION

HN1 is an oncogene previously shown as overexpressed in many cancers.[7,11,41–43] In a glioma model, HN1 was involved in advanced tumorigenesis or malignant tumors of the brain.[41] Here, we showed that HN1 is significantly overexpressed in neuroblastoma samples as compared to control counterparts (Figure 1). Moreover, it was discovered that *HN1* levels remained lower in PD and RA-differentiated SH-SY5Y cells using bioinformatics analysis. SH-SY5Y cells were differentiated using RA treatments and HN1 levels were confirmed as lower upon RA-differentiation. Furthermore, *HN1* coexpression network analysis was performed to find the putative pathways of *HN1*-related genes as described previously.[15] The cell cycle pathways are enriched in the network and HN1 levels remain higher in the S-phase of the cell cycle (Figure 2). Recently, it was established that HN1 levels are enriched in S-phase with phosphorylation form appearing in mitosis.[16] Therefore, the present data complies with previous reports.

HN1 overexpression changes cell cycle distribution in prostate cancer cells, where S-phase accumulation has been reported,[15,16] however in neuroblastoma cells (SH-SY5Y), HN1 overexpression increased accumulation

in G2-M phase (Figure 3) in both undifferentiated and RA-differentiated SH-SY5Y cells (Figure S1). This data indicates that HN1 is a cell cycle regulatory factor in neuronal progenitors, as neurons are postmitotic and HN1 expression is enriched in S-phase. In prostate cancer cells, HN1 inhibits the Akt-mediated GSK3β signaling via direct interactions with S9-phosphorylated GSK3β.[44] HN1 also inhibited the β-catenin via proteasomal degradation and influenced the β-catenin-E-cadherin interaction negatively, leading to an invasive migratory profile in Prostate cancer cells with cytoskeletal reorganization.[12] Here, we showed that HN1 overexpression increases GSK3β in undifferentiated SH-SY5Y cells but GSK3β inhibition stabilizes HN1 in both undifferentiated and RA-differentiated SH-SY5Y cells. Furthermore, HN1 interacts with GSK3β to stabilize MYC to induce tumorigenesis in hepatocellular carcinoma, where it is considered a potential target for therapy.[45] GSK3β is one of the upstream kinases of β-catenin as well as HN1.[16] Therefore, in RA-differentiation, HN1 inhibition could be the result of GSK3β activity as GSK3β inhibition has been established as a major mechanism of inhibition of RA-mediated differentiation of SH-SY5Y cells.[31]

HN1 overexpression resulting in the reduction of mature neuronal marker GAP43 (Figure 3)[23,46] is strong evidence that HN1 plays a role in dedifferentiation of neurons. Furthermore, HN1 overexpression promoted the expression of Cdk2 and enhanced Skp2, leading to the progression of cell cycle in RA-differentiated cells as well. HN1 also interacts with Stathmin 1, which acts as a microtubule destabilizing protein, reduces acetylation of α-tubulin and increases the epithelial–mesenchymal-transition in ATC.[13] Here, we showed that in undifferentiated SH-SY5Y cells, HN1 overexpression increased acetyl-α-tubulin and decreased it in RA-differentiated SH-SY5Y cells suggesting that the HN1 has a regulatory role in balancing differentiation and progression of the cell cycle (Figure 3). Moreover, HN1 levels were correlated with microtubule dynamics in SH-SY5Y cells (Figure 4), indicating that HN1 is regulated via cytoskeletal factors as well. RA treatment also led to the accumulation of β-catenin in the nucleus in SH-SY5Y cells (Figure 5), without significant change with HN1 expression, suggesting that the HN1 has a role in dedifferentiation of SH-SY5Y cells through cell cycle regulation.[31] Moreover, HN1 overexpression increased the S-type SH-SY5Y populations, demonstrating a dedifferentiation phenotype. Therefore, HN1 is clearly involved in the dedifferentiation of SH-SY5Y cells via cell cycle regulation and microtubule dynamics. Further mechanistic insights are required to understand the role of HN1 in these mechanisms.

5 | CONCLUSION

This is the first report investigating HN1 in the context of neuroblastoma or RA-differentiated SH-SY5Y cells. We discovered that HN1 levels are enriched in S-phase and correlates with dedifferentiation of neurons. Moreover, RA induction of differentiation downregulates HN1 significantly. The expression of HN1 is also associated with microtubule dynamics. HN1 overexpression leads to change in cell cycle distribution as evident in increased G2-M populations and geminin levels. Nuclear accumulation of β-catenin in RA-differentiated cells upon HN1 overexpression demonstrates the role of HN1 in dedifferentiation of neuroblastoma cells.

ACKNOWLEDGMENTS

The authors acknowledge Prof. Dr. Ayşe Nalbantsoy for providing access to BD Accuri C6 Flowcytometer. This research was funded with Ege University BAP Project (internal grant number FGA-23341), and TÜBİTAK Project 221Z202 to Kemal S. Korkmaz.

CONFLICT OF INTEREST STATEMENT

The authors declare no conflict of interest.

DATA AVAILABILITY STATEMENT

The data that support the findings of this study are available from the corresponding author upon reasonable request. Data openly available in a public repository that issues datasets with DOIs is mentioned with names of the respective datasets.

ORCID

Tilbe Özar http://orcid.org/0000-0001-8682-7428
Gülseren Özduman http://orcid.org/0000-0002-6019-3268
Kemal S. Korkmaz http://orcid.org/0000-0003-4040-2568

REFERENCES

1. Tang W, Lai YH, Han XD, Wong PMC, Peters LL, Chui DHK. Murine Hn1 on chromosome 11 is expressed in hemopoietic and brain tissues. *Mamm Genome*. 1997;8:695-696. doi:10.1007/s003359900540
2. Zujovic V, Luo D, Baker HV, et al. The facial motor nucleus transcriptional program in response to peripheral nerve injury identifies Hn1 as a regeneration-associated gene. *J Neurosci Res*. 2005;82:581-591. doi:10.1002/jnr.20676
3. Goto T, Hisatomi O, Kotoura M, Tokunaga F. Induced expression of hematopoietic- and neurologic-expressed sequence 1 in retinal pigment epithelial cells during newt retina regeneration. *Exp Eye Res*. 2006;83:972-980. doi:10.1016/j.exer.2006.05.004

4. Laughlin KM, Luo D, Liu C, et al. Hematopoietic- and neurologic-expressed sequence 1 (Hn1) depletion in B16.F10 melanoma cells promotes a differentiated phenotype that includes increased melanogenesis and cell cycle arrest. *Differentiation*. 2009;78(1):35-44. doi:10.1016/j.diff.2009.04.001
5. Goto T, Tokunaga F, Hisatomi O. Hematological- and neurological-expressed sequence 1 gene products in progenitor cells during newt retinal development. *Stem Cells Int*. 2012;2012:1-6. doi:10.1155/2012/436042
6. Zhou G, Wang J, Zhang Y, et al. Cloning, expression and subcellular localization of HN1 and HN1L genes, as well as characterization of their orthologs, defining an evolutionarily conserved gene family. *Gene*. 2004;331:115-123. doi:10.1016/j.gene.2004.02.025
7. Zhang C, Xu B, Lu S, Zhao Y, Liu P. HN1 contributes to migration, invasion, and tumorigenesis of breast cancer by enhancing MYC activity. *Mol Cancer*. 2017;16(1):90. doi:10.1186/s12943-017-0656-1
8. Zhang ZG, Chen WX, Wu YH, Liang HF, Zhang BX. MiR-132 prohibits proliferation, invasion, migration, and metastasis in breast cancer by targeting HN1. *Biochem Biophys Res Commun*. 2014;454:109-114. doi:10.1016/j.bbrc.2014.10.049
9. Pu J, Wang J, Li W, et al. hsa_circ_0000092 promotes hepatocellular carcinoma progression through up-regulating HN1 expression by binding to microRNA-338-3p. *J Cell Mol Med*. 2020;28:e15010. doi:10.1111/jcmm.15010
10. Wang R, Fu Y, Yao M, et al. The HN1/HMGB1 axis promotes the proliferation and metastasis of hepatocellular carcinoma and attenuates the chemosensitivity to oxaliplatin. *FEBS J*. 2022;289(20):6400-6419.
11. Chen JJ, Sun X, Mao QQ, et al. Increased expression of hematological and neurological expressed 1 (HN1) is associated with a poor prognosis of hepatocellular carcinoma and its knockdown inhibits cell growth and migration partly by down-regulation of c-Met. *Kaohsiung J Med Sci*. 2020;36(3):196-205. doi:10.1002/kjm2.12156
12. Varisli L, Ozturk BE, Akyuz GK, Korkmaz KS. HN1 negatively influences the β-catenin/E-cadherin interaction, and contributes to migration in prostate cells. *J Cell Biochem*. 2015;116:170-178. doi:10.1002/jcb.24956
13. Pan Z, Fang Q, Li L, et al. HN1 promotes tumor growth and metastasis of anaplastic thyroid carcinoma by interacting with STMN1. *Cancer Lett*. 2021;501:31-42.
14. Chen J, Qiu J, Li F, et al. HN1 promotes tumor associated lymphangiogenesis and lymph node metastasis via NF-κB signaling activation in cervical carcinoma. *Biochem Biophys Res Commun*. 2020;530(1):87-94. doi:10.1016/j.bbrc.2020.05.062
15. Varisli L, Javed A, Ozturk BE, et al. HN1 interacts with γ-tubulin to regulate centrosomes in advanced prostate cancer cells. *Cell Cycle*. 2021;20(17):1723-1744. doi:10.1080/15384101.2021.1962624
16. Javed A, Özduman G, Varışlı L, Öztürk BE, Korkmaz KS. HN1 is enriched in the S-phase, phosphorylated in mitosis, and contributes to cyclin B1 degradation in prostate cancer cells. *Biology*. 2023;12(2):189.
17. Pan Z, Lu X, Xu T, et al. Epigenetic inhibition of CTCF by HN1 promotes dedifferentiation and stemness of anaplastic thyroid cancer. *Cancer Lett*. 2024;580:216496.
18. Shipley MM, Mangold CA, Szpara ML. Differentiation of the SH-SY5Y human neuroblastoma cell line. *J Visualized Exp*. 2016;108:53193. doi:10.3791/53193
19. Magalingam KB, Radhakrishnan AK, Somanath SD, Md S, Haleagrahara N. Influence of serum concentration in retinoic acid and phorbol ester induced differentiation of SH-SY5Y human neuroblastoma cell line. *Mol Biol Rep*. 2020;47:8775-8788. doi:10.1007/s11033-020-05925-2
20. Xie HR, Hu LS, Li GY. SH-SY5Y human neuroblastoma cell line: in vitro cell model of dopaminergic neurons in Parkinson's disease. *Chin Med J*. 2010;123(8):1086-1092.
21. Kovalevich J, Santerre M, Langford D. Considerations for the use of SH-SY5Y neuroblastoma cells in neurobiology. *Methods Mol Biol*. 2021;1078:9-21.
22. Cheung YT, Lau WKW, Yu MS, et al. Effects of all-trans-retinoic acid on human SH-SY5Y neuroblastoma as in vitro model in neurotoxicity research. *Neurotoxicology*. 2009;30:127-135. doi:10.1016/j.neuro.2008.11.001
23. Encinas M, Iglesias M, Liu Y, et al. Sequential treatment of SH-SY5Y cells with retinoic acid and brain-derived neurotrophic factor gives rise to fully differentiated, neurotrophic factor-dependent, human neuron-like cells. *J Neurochem*. 2000;75:991-1003. doi:10.1046/j.1471-4159.2000.0750991.x
24. Bartha Á, Győrffy B. Tnmplot.Com: a web tool for the comparison of gene expression in normal, tumor and metastatic tissues. *Int J Mol Sci*. 2021;22:2622. doi:10.3390/ijms22052622
25. Sun Y, Ye L, Zheng Y, Yang Z. Identification of crucial genes associated with Parkinson's disease using microarray data. *Mol Med Rep*. 2018;17:3775-3882. doi:10.3892/mmr.2017.8305
26. Gao J, Aksoy BA, Dogrusoz U, et al. Integrative analysis of complex cancer genomics and clinical profiles using the cBioPortal. *Sci Signal*. 2013;6(269):pl1. doi:10.1126/scisignal.2004088
27. Moran LB, Graeber MB. Towards a pathway definition of Parkinson's disease: a complex disorder with links to cancer, diabetes and inflammation. *Neurogenetics*. 2008;9:1-13. doi:10.1007/s10048-007-0116-y
28. Nishida Y, Adati N, Ozawa R, Maeda A, Sakaki Y, Takeda T. Identification and classification of genes regulated by phosphatidylinositol 3-kinase- and TRKB-mediated signalling pathways during neuronal differentiation in two subtypes of the human neuroblastoma cell line SH-SY5Y. *BMC Res Notes*. 2008;1:95. doi:10.1186/1756-0500-1-95
29. Fonseka P, Pathan M, Chitti SV, Kang T, Mathivanan S. FunRich enables enrichment analysis of OMICs datasets. *J Mol Biol*. 2021;433:166747. doi:10.1016/j.jmb.2020.166747
30. Sarkanen JR, Nykky J, Siikanen J, Selinummi J, Ylikomi T, Jalonen TO. Cholesterol supports the retinoic acid-induced synaptic vesicle formation in differentiating human SH-SY5Y neuroblastoma cells. *J Neurochem*. 2007;102:1941-1952. doi:10.1111/j.1471-4159.2007.04676.x
31. Lin CC, Chou CH, Howng SL, et al. GSKIP, an inhibitor of GSK3β, mediates the N-cadherin/β-catenin pool in the differentiation of SH-SY5Y cells. *J Cell Biochem*. 2009;108:1325-1336. doi:10.1002/jcb.22362
32. Wang HY, Juo LI, Lin YT, et al. WW domain-containing oxidoreductase promotes neuronal differentiation via negative regulation of glycogen synthase kinase 3B. *Cell Death Differ*. 2012;19:1049-1059. doi:10.1038/cdd.2011.188

33. Darshit BS, Ramanathan M. Activation of AKT1/GSK-3β/β-catenin–TRIM11/survivin pathway by novel GSK-3β inhibitor promotes neuron cell survival: study in differentiated SH-SY5Y cells in OGD model. *Mol Neurobiol*. 2016;53:6716-6729. doi:10.1007/s12035-015-9598-z
34. López-Carballo G, Moreno L, Masiá S, Pérez P, Barettino D. Activation of the phosphatidylinositol 3-kinase/Akt signaling pathway by retinoic acid is required for neural differentiation of SH-SY5Y human neuroblastoma cells. *J Biol Chem*. 2002;277:25297-25304. doi:10.1074/jbc.M201869200
35. Wiedmer L, Ducray AD, Frenz M, Stoffel MH, Widmer HR, Mevissen M. Silica nanoparticle-exposure during neuronal differentiation modulates dopaminergic and cholinergic phenotypes in SH-SY5Y cells. *J Nanobiotechnol*. 2019;17:46. doi:10.1186/s12951-019-0482-2
36. Singh US, Pan J, Kao YL, Joshi S, Young KL, Baker KM. Tissue transglutaminase mediates activation of RhoA and MAP kinase pathways during retinoic acid-induced neuronal differentiation of SH-SY5Y cells. *J Biol Chem*. 2003;278:391-399. doi:10.1074/jbc.M206361200
37. Arendt T. Differentiation and de-differentiation—neuronal cell-cycle regulation during development and age-related neurodegenerative disorders. In: Lajtha A, Perez-Polo JR, Rossner S, eds. *Handbook of Neurochemistry and Molecular Neurobiology*. Springer; 2008;160-213.
38. Cuende J, Moreno S, Bolaños JP, Almeida A. Retinoic acid downregulates Rae1 leading to APCCdh1 activation and neuroblastoma SH-SY5Y differentiation. *Oncogene*. 2008;27:3339-3344. doi:10.1038/sj.onc.1210987
39. Filograna R, Civiero L, Ferrari V, et al. Analysis of the catecholaminergic phenotype in human SH-SY5Y and BE(2)-M17 neuroblastoma cell lines upon differentiation. *PLoS One*. 2015;10:e0136769. doi:10.1371/journal.pone.0136769
40. Bell N, Hann V, Redfern CPF, Cheek TR. Store-operated Ca2+ entry in proliferating and retinoic acid-differentiated N- and S-type neuroblastoma cells. *Biochim Biophys Acta*. 2013;1833:643-651. doi:10.1016/j.bbamcr.2012.11.025
41. Laughlin KM, Luo D, Liu C, et al. Hematopoietic- and neurologic-expressed sequence 1 expression in the murine GL261 and high-grade human gliomas. *Pathol Oncol Res*. 2009;15:437-444. doi:10.1007/s12253-008-9147-4
42. Lu KH, Patterson AP, Wang L, et al. Selection of potential markers for epithelial ovarian cancer with gene expression arrays and recursive descent partition analysis. *Clin Cancer Res*. 2004;10:3291-3300. doi:10.1158/1078-0432.CCR-03-0409
43. Tang Y, Zhang Z, Tang Y, Chen X, Zhou J. Identification of potential target genes in pancreatic ductal adenocarcinoma by bioinformatics analysis. *Oncol Lett*. 2018;16:2453-2461. doi:10.3892/ol.2018.8912
44. Varisli L, Gonen-Korkmaz C, Debelec-Butuner B, et al. Ubiquitously expressed hematological and neurological expressed 1 downregulates Akt-mediated GSK3β signaling, and its knockdown results in deregulated G2/M transition in prostate cells. *DNA Cell Biol*. 2011;30(6):419-429. doi:10.1089/dna.2010.1128
45. Feng J, Liu Y, Fang T, Zhu J, Wang G, Li J. Hematological and neurological expressed 1 (HN1) activates c-Myc signaling by inhibiting ubiquitin-mediated proteasomal degradation of c-Myc in hepatocellular carcinoma. *Cell Biol Int*. 2023;47:560-572. doi:10.1002/cbin.11957
46. Do CB, Jaiswal MS, Jang YS, Kim UK, Kim GC, Hwang DS. Non-thermal plasma directly accelerates neuronal proliferation by stimulating axon formation. *Sci Rep*. 2022;12:15868. doi:10.1038/s41598-022-20063-4

SUPPORTING INFORMATION

Additional supporting information can be found online in the Supporting Information section at the end of this article.

How to cite this article: Özar T, Javed A, Özduman G, Korkmaz KS. HN1 is a novel dedifferentiation factor involved in regulating the cell cycle and microtubules in SH-SY5Y neuroblastoma cells. *J Cell Biochem*. 2025;126:e30569. doi:10.1002/jcb.30569